TRIPLE COLLOCATION OF SUMMER PRECIPITATION RETRIEVALS FROM SEVIRI OVER EUROPE WITH GRIDDED RAIN GAUGE AND WEATHER RADAR DATA

R. A. Roebeling[1,2], E.L.A. Wolters[1], J.F. Meirink[1] and H. Leijnse[1]

[1] Royal Netherlands Meteorological Institute (KNMI) P.O. Box 201, 3730 AE De Bilt, The Netherlands

[2] EUMETSAT, Eumetsat Allee 1, D-64295, Darmstadt, Germany

Corresponding author:

R. A. Roebeling

EUMETSAT,

Eumetsat Allee 1,

D-64295 Darmstadt,

Germany.

Tel : +49 (0) 6151 807-0

Email : rob.roebeling@eumetsat.int

ABSTRACT

Quantitative information on the spatial and temporal error structures in large-scale (regional or global) precipitation data sets is essential for hydrologic and climatic studies. A powerful tool to quantify error structures in large-scale data sets is triple collocation.

In this paper, triple collocation is used to determine the spatial and temporal error characteristics of three precipitation data sets over Europe, i.e., the Precipitation Properties Visible Near InfraRed (PP-VNIR) retrievals from the Spinning Enhanced Visible and Infrared Imager (SEVIRI) instrument onboard Meteosat Second Generation (MSG), weather radar observations from the European integrated weather radar system, and gridded rain gauge observations from the Global Precipitation Climatology Centre (GPCC) and the European Climate Assessment and Dataset (ECA&D) data sets. For these data sets the spatial and temporal error characteristics are evaluated and their performance is discussed. Finally, weather radar and PP-VNIR retrievals are used to evaluate the diurnal cycles of precipitation occurrence and intensity during daylight hours for different European climate regions.

The results suggest that the triple collocation method provides realistic error estimates. The spatial and temporal error structures agree with the findings of earlier studies, and reveal the strengths and weaknesses of the data sets, such as the effect of morphological variations in weather radar data set, the effect of sampling density in the gridded rain gauge data set, and the sensitivity to retrieval assumptions in the PP-VNIR data set. This study can help us in developing adequate strategies for combining various precipitation data sets, for example for improved monitoring of diurnal variations or for detecting temporal trends in precipitation.

Introduction

Accurate information on spatial and temporal variations in precipitation occurrence (areal or temporal fraction at which precipitation occurs) and intensity (rain rates) is of great importance for evaluating precipitation parameterizations in weather and climate models, and for studying feedbacks between precipitation and atmospheric or surface quantities. These studies require information at high spatial and temporal resolutions. Although operational weather radars provide information on precipitation occurrence and intensity and the networks of these radars are expanding over Europe and the United States, large areas of the world remain undersampled or are not sampled at all (e.g. ocean). Passive imagers operated on geostationary satellites can bridge this gap and provide quasi-global information on the occurrence and intensity of precipitation.

Over the past decades, several methods have been developed to detect precipitating clouds and retrieve rain rates from passive imagers (Kidd and Levizzani, 2011). The methods developed for geostationary satellites often use thermal infrared observations, and relate daily minimum cloud top temperatures (Adler and Negri, 1988) or Cold Cloud Durations (CCD) to rain rates (Todd et al., 1995). The infrared-based methods give fair accuracies over areas where rainfall is governed by deep convection. Several methods have been developed to detect precipitating clouds from cloud physical properties retrieved from passive imagers (Rosenfeld and Gutman, 1994; Lensky and Rosenfeld, 2006; Nauss and Kokanovsky, 2006; Thies et al., 2008 and Roebeling and Holleman, 2009). These methods exploit the information that can be derived from the observed reflection in the non-absorbing visible channels (0.6 or 0.8 μm), which is primarily a function of the cloud optical thickness, and the absorbing near-infrared channels (1.6, 2.1 or 3.8 μm), which is primarily a function of cloud particle size. Roebeling and Holleman (2009) developed a cloud microphysics based algorithm to retrieve precipitation occurrence and intensity named the

Precipitation Properties Visible and Near InfraRed (PP-VNIR) algorithm. Although their algorithm only requires visible and near-infrared observations from passive imagers, it combines two physical approaches that have been developed for visible and near-infrared observations and for Microwave Radiometer (MWR) observations, respectively. The approach to retrieve precipitation occurrence is taken from Lensky and Rosenfeld (2006), which was developed for visible and near-infrared observations. The approach to retrieve precipitation intensity is taken from Wentz and Spencer (1998), which was developed for MWR observations. Wolters et al. (2011) validated the PP-VNIR algorithm over West Africa against Tropical Rainfall Measuring Mission Precipitation Radar (TRMM-PR) and Climate Prediction Center Morphing Method (CMORPH) observations. It was found that in general the difference between the PP-VNIR and TRMM-PR rain rates is within +/- 10%. In addition, it was shown that the PP-VNIR algorithm is well suitable for monitoring the daytime diurnal cycle of precipitation in tropical areas.

The retrieval of precipitation intensities for stratiform and convective clouds is feasible with the more physically-based satellite MWR retrieval methods (e.g. Wentz and Spencer, 1998) that relate retrieved liquid water path and rain column height to precipitation intensity. The main drawbacks of the MWR-based retrievals are that they only apply to liquid precipitation and are only available from polar orbiting satellites, and hence have a very limited time resolution. Recent studies attempt to exploit MWR observations for solid precipitation retrievals as well. The way forward, however, is complex as it requires a multi-sensor approach combining active and passive instrument observations, as well as a need to increase our physical understanding of the microphysical and radiative properties of ice hydrometeors (Levizzani et al., 2011; Grecu and Olson, 2008).

Beside single instrument retrievals, methods have been developed that combine measurement from different sources. The CMORPH method provides global precipitation estimates by propagating motion vectors derived from geostationary satellite infrared observations on passive microwave satellite scans (Joyce et al., 2004). The Global Precipitation Climatology Project (GPCP, Adler et al., 2003) merges measurements from three different sources, i.e., precipitation estimates from low-orbit satellite microwave data, geosynchronous-orbit satellite infrared data, and surface gauge precipitation observations from the Global Precipitation Climatology Centre (GPCC, Rudolf et al., 2011). The Precipitation Estimation from Remotely Sensed Information using Artificial Neural Networks (PERSIANN) combines information from infrared and microwave satellite imagery, and ground-surface topography to estimate precipitation, whereas rain gauge and weather radar data are used for calibration (Hsu et al., 1997). Because most combined precipitation products are tuned towards rain gauge observations, their bias with respect to these observations is small. However, combining information from different sources with different temporal and spatial resolutions will change the statistics of the precipitation data sets, which makes them less suited for evaluating the probability density functions of precipitation as is done in studies of, for example, extreme statistics.

Frequent observations of precipitation occurrence and intensity are needed to evaluate and improve model predictions of precipitation. Weather radars and geostationary satellites can provide these observations at the required spatial and temporal scales. This paper aims to determine the applicability of precipitation retrievals from the European network of weather radars and from the PP-VNIR algorithm using observations from the Spinning Enhanced Visible and Infrared Imager (SEVIRI) for climate and weather model evaluation studies. First, the ability of the weather radar and PP-VNIR retrievals to capture spatial and temporal variations in precipitation over Europe is determined. Hereto, we will perform a triple collocation analysis between these retrievals and the GPCC and/or the European Climate Assessment and Data set (ECA&D) gridded rain gauge data for the summer months of 2005, 2006, and 2007. Second, our study will analyze whether the precipitation occurrence and intensity retrievals of weather radars and the PP-VNIR algorithm reveal similar diurnal cycles during daylight hours, so as to determine their applicability for evaluating corresponding diurnal cycles predicted by weather and climate models.

The outline of this paper is as follows. In Section 2, the satellite, weather radar and ground-based measurements and retrieval methods are presented. In Section 3, the triple collocation method is explained. The results of the triple collocation for the summer months of 2005, 2006, and 2007 are presented in Section 4. The applicability of weather radar observations and PP-VNIR retrievals is further discussed in Section 5. Finally, in Section 6, a summary is given and conclusions are drawn.

1. Measurements and methods

a. Satellite observations

Meteosat Second Generation (MSG) is a series of European geostationary satellites that are operated by the European Organisation for the Exploitation of Meteorological Satellites (EUMETSAT). The first MSG satellite (METEOSAT-8) was successfully launched in August 2002, while in December 2005 the second MSG satellite (METEOSAT-9) was launched. The MSG is a spinning stabilized satellite that is positioned at an altitude of about 36000 km above the equator at 3.4° W for METEOSAT-8 and 0.0° for METEOSAT-9. The SEVIRI instrument scans Europe and Africa every 15 minutes and operates three channels at visible and near-infrared wavelengths between 0.6 and 1.6 μm, eight channels at infrared wavelengths between 3.8 and 14 μm, and one high-resolution visible channel at 0.7 μm. The nadir spatial resolution of SEVIRI is 1×1 km^2 for the broadband high-resolution channel and 3×3 km^2 for the other channels. Over Northern Europe (the Netherlands) the satellite viewing zenith angle of SEVIRI is about 60° and as a consequence the spatial resolution is reduced to about 4×7 km^2.

b. Satellite retrievals

The Cloud Physical Properties (CPP) algorithm of the Satellite Application Facility on Climate Monitoring (CM-SAF) is used to retrieve Cloud Phase (*CPH*), Cloud Optical Thickness (*COT*), particle size (r_e), and Condensed Water Path (*CWP*) from SEVIRI reflectances (Roebeling et al., 2006). *COT* and r_e are retrieved for cloudy pixels in an iterative manner by simultaneously comparing satellite-observed reflectances at visible (0.6 μm) and near-infrared (1.6 μm) wavelengths with Look Up Tables (LUTs) of reflectances calculated for water and ice clouds with given optical thicknesses, particle sizes and surface albedos. The LUTs have been generated with the Doubling Adding KNMI (DAK) radiative transfer model (De Haan et al., 1987; Stammes, 2001). The retrieval of *CPH* is done simultaneously with the retrieval of *COT* and particle size. The phase “ice” is assigned to pixels for which the observed 0.6 μm and 1.6 μm reflectances correspond to simulated reflectances of ice clouds, and the cloud-top temperature is lower than 265 K. The remaining cloudy pixels are considered to represent water clouds (Wolters et al., 2008). The *CWP* is computed from the retrieved *COT* and particle size. The retrievals are limited to satellite and solar viewing zenith angles smaller than 72°. Varnai and Marshak (2007) found that cloud property retrievals become more sensitive to errors with increasing satellite and solar viewing zenith angles as a result of larger inaccuracies in the radiative transfer simulations, lower signal-to-noise ratio of the reflectance observations, and larger differences between one-dimensional and three-dimensional cloud reflectances. In addition, Roebeling et al. (2008) showed that the uncertainties in COT retrievals increase with increasing visible reflectances, which saturate at high COT values.

PP-VNIR is a cloud microphysics-based algorithm for the retrieval of precipitation occurrence and intensity from passive imager observations (Roebeling and Holleman, 2009). Precipitation occurrence is retrieved from information on *CWP*, *CPH*, and droplet effective radius using three detection criteria. First, clouds with *CWP* values larger than a threshold value (CWP_T) are considered potentially precipitating. Second, information on *CPH* is used to separate ice from water clouds. All ice clouds with *CWP* values larger than CWP_T are labeled precipitating. Third, information on the droplet effective radius is used to separate precipitating from non-precipitating water clouds. All water clouds with a droplet effective radius larger than a threshold value (r_{eT}) and *CWP* values larger than CWP_T are labeled precipitating. Precipitation intensity (*R*) is retrieved from information on *CWP* and height of the rain column (*H*) using the following equation:

$$R = \frac{c}{H}\left[\frac{CWP - CWP_0}{CWP_0}\right]^{\alpha} \qquad (1)$$

where *R* is given in mm h^{-1} and *H* is given in km, CWP_0 is the *CWP* offset value in g m^{-2} above which *R* is calculated, α is a dimensionless constant, and *c* is a constant in mm h^{-1} km that has a value of 1. The retrieved rain intensities are limited to a maximum intensity ($R_{\max}$). Inspired by the empirical relationship between R and CTT suggested by Vicente et al. (1998), we calculate $R_{\max}$ as function of H and an offset rain intensity (R_0) with the following equation:

$$R_{\max} = R_0 + H^{1.6} \tag{2}$$

To reduce the impact of $R_{\max}$ on our precipitation retrievals R_0 is chosen to be conveniently large and set at 2 mm hr^{-1}. H is determined from the difference between the highest cloud-top temperature over an area of 100×100 SEVIRI pixels ($CTT_{\max}$), which is assumed to represent a thin water cloud with a minimum rain column height (dH), and the cloud top temperature of the observed pixel (CTT_{pix}). Assuming that the vertical decrease in temperature obeys a wet adiabatic lapse rate of 6.5 K km^{-1}, H can be derived as follows:

$$H = \frac{(CTT_{\max} - CTT_{pix})}{6.5} + dH \tag{3}$$

Roebeling and Holleman (2009) calibrated the PP-VNIR algorithm over the Netherlands with weather radar observations yielding the following optimum settings for: CWP_T (160 g m^{-2}), r_{eT} (15 μm) , CWP_0 (120 g m^{-2}), α (1.6), and dH (0.6 km). PP-VNIR retrievals have been validated over the Netherlands against weather radar observations (Roebeling and Holleman, 2009) and over West Africa against TRMM-PR observations (Wolters et al., 2011), which revealed that these retrievals have an accuracy of about 0.8 mm h^{-1} and a precision of about 1.0 mm h^{-1}.

c. Weather radar observations

The EUMETNET Operational Programme for the Exchange of weather RAdar information (OPERA) is an ongoing European program that provides a platform to exchange expertise on operational weather radar issues and to harmonize and improve the operational exchange of weather radar information between national meteorological services (e.g. Huuskonen, 2006; Holleman et al., 2008; Huuskonen et al., 2010). An important achievement of OPERA is the establishment of the exchange of weather radar data through a data hub. Current work of OPERA is focused on the harmonization and quality control and improvement of radars across Europe. The radar data used in this study is a composite of the national composites of 6 countries: Belgium (2), France (23), Germany (16), Ireland (2), Netherlands (2), and United Kingdom (14). This means that the radar data used in this paper is a European composite based on a network of 59 radars distributed over Western Europe. It should be noted that this network comprises different types of radars i.e., the majority are C-band radars (with some S-band radars), most of which are Doppler radars, and some are dual polarization radars. The European composite is provided as dBZ values, which are observed every 5 minutes at a horizontal resolution of 4×4 km^2. More details on the radar network used in this study can be found in Huuskonen (2006).

Note that weather radar retrievals are not without problems, and are subject to numerous uncertainties, including calibration, attenuation, beam blockage, ground clutter, or variations in the relation between the radar echoes and rainfall rate (e.g. Wilson and Brandes, 1979; Krajewski et al., 2010; Hazenberg et al., 2011). Weather radar observations are only quantitatively usable for the central part of the image, covering an area of about 200 km around the weather radar station. Due to the Earth's curvature, the distance over which weather radars observe the entire cloud is limited and at KNMI a maximum range of 200 km is used for quantitative precipitation estimation (Overeem et al., 2009).

Weather radars employ backscattering of radio-frequency waves (5.6 GHz for C-band) to measure precipitation and other particles in the atmosphere (e.g. Battan, 1973; Doviak and Zrnic, 1993). The intensity of the atmospheric echoes is converted to the so-called radar reflectivity factor (Z) using the Rayleigh-scattering approximation. This approximation is valid when the radar wavelength (5 cm) is much larger than the raindrop diameters (<6 mm). Radar reflectivity factors are converted to rainfall intensities (R) using a fixed power law (Marshall et al., 1955):

$$Z = 200 R^{1.6} \tag{4}$$

with the radar reflectivity factor Z in mm^6 m^{-3} and rainfall intensity R in mm h^{-1}.

d. GPCC and E-OBS data sets

Gauge-based gridded precipitation data sets are another source of information. For Europe the two most widely used gauge-based gridded data sets are the GPCC data set provided by the German Weather Service (Rudolf et al., 2011) and the European Daily High-resolution Observational Gridded Dataset (E-OBS) provided by the Royal Netherlands Meteorological Institute (Haylock et al., 2008).

The GPCC data set is available at a regular grid of 0.5°, 1.0° or 2.5° at a monthly resolution. This data set covers the global land areas excluding Greenland and Antarctica over a period of more than 100 years (1901 to 2009), and is freely available for scientific purposes (http://gpcc.dwd.de). This gridded data set is generated from the most comprehensive station database of monthly observed precipitation world-wide. The amount of available stations varies with time, and reached a maximum of ca. 45000 stations globally in 1986/87. Over Europe the number of observing stations is larger than 7000. These stations are unevenly distributed, with the highest densities in the Germany, France, the UK, the Netherlands and Switzerland. All observations in this database are subject to a multi-stage quality control to minimize the risk of generating temporal inhomogeneities in the gridded data due to varying station densities. Hereafter the data are projected on a regular grid by spatially interpolating the anomalies from climatological normals at the stations using a modified version of the Spheremap method (Willmott et al., 1985), and super-imposing these gridded anomalies on the background climatology. For our study we used the GPCC Full Data Reanalysis Product version 4 of monthly precipitation amounts projected at regular grid of 0.5°x0.5°.

The European Daily High-resolution Observational Gridded Dataset (E-OBS) of rain gauge observations is available on a regular grid of 0.25°×0.25° and at a daily resolution. The daily observations at point locations are taken from the European Climate Assessment and Dataset (ECA&D; http://eca.knmi.nl) comprising a set of about 2300 observing stations. These stations are unevenly distributed, with the highest densities in the UK, the Netherlands and Switzerland. E-OBS provides land-only information on precipitation amounts and minimum, maximum, and mean surface temperatures over Europe for the period 1950–2006 (Haylock et al, 2008). This data set improves on previous products in its spatial resolution and extent, time period, number of contributing stations, and attention to find the most appropriate method for spatial interpolation of daily climate observations. The data set has been designed to provide the best estimate of grid box averages rather than point values to enable direct comparisons with regional climate models. The interpolation process is employed in three steps. First, the monthly precipitation totals and monthly mean temperature are interpolated using three-dimensional thin-plate splines. Second, the daily anomalies are interpolated using indicator and universal kriging for precipitation and kriging with an external drift for temperature. Finally, the monthly and daily estimates are combined. Interpolation uncertainty is quantified by the provision of daily standard errors for every grid square.

2. Triple collocation

Triple collocation is a method that can be used to estimate the errors and the cross-calibration of three linearly related data sets with uncorrelated errors (Stoffelen et al., 1998). Until now, triple collocation has been mainly applied for error estimates and calibration of scatterometer winds (Stoffelen et al., 1998; Jansen et al., 2007) and soil moisture retrievals (Scipal et al, 2008; Dorigo et al., 2010). However, triple collocation can be applied to all types of physical parameters that represent the same spatial and temporal scales, and are subject to mean random errors with a Gaussian nature. In this paper, the method is applied to quantify the residual errors in three independent precipitation data sets. Below we will introduce the general principles of the triple collocation method.

Triple collocation assumes that the rainfall data sets *(R_x)* are related to a hypothetical true precipitation (R) as follows (Stoffelen et al, 1998):

$$\begin{aligned} R_g &= \alpha_g + \beta_g R + e_g \\ R_r &= \alpha_r + \beta_r R + e_r \\ R_s &= \alpha_s + \beta_s R + e_s \end{aligned} \tag{5}$$

in which α_x are the offsets, β_x the gains and e_x the residual errors. Here x represents the gridded rain gauge (*g*), weather radar (*r*), and satellite (*s*) data sets, respectively. To eliminate differences due to differences in the α_{x} and β_{x}, the three data sets are recalibrated to the hypothetical true precipitation *R*. The recalibrated data sets are defined as $R_x^* = R + e_x^*$, which are calculated by eliminating the calibration coefficients in the observational data sets $R_x^* = R_x / \beta_x - \alpha_x / \beta_x$ and in the residual errors $e_x^* = e_x / \beta_x$. Because the hypothetical true precipitation is not known, one of the three data sets is chosen as a reference. The residual errors do not depend on the chosen reference data set. Now the unknown true precipitation can be removed, and Eq. 5 can be rewritten to:

$$\begin{aligned} R_g^* - R_r^* &= e_g^* - e_r^* \\ R_g^* - R_s^* &= e_g^* - e_s^* \\ R_r^* - R_s^* &= e_r^* - e_s^* \end{aligned} \tag{6}$$

By cross-multiplying the equations of Eq. 6 and assuming that the residual errors are uncorrelated, the mean variance of residual errors ($\left\langle e_x^{*2} \right\rangle$) can be fully determined by three independent and calibrated precipitation estimates using the following equations:

$$\begin{aligned} \left\langle e_{g'}^{*2} \right\rangle &= \left\langle (R_g^* - R_r^*)(R_g^* - R_s^*) \right\rangle \\ \left\langle e_{r'}^{*2} \right\rangle &= \left\langle (R_r^* - R_g^*)(R_r^* - R_s^*) \right\rangle \\ \left\langle e_{s'}^{*2} \right\rangle &= \left\langle (R_s^* - R_g^*)(R_s^* - R_r^*) \right\rangle \end{aligned} \tag{7}$$

The triple collocation errors that are evaluated in this paper are $\left\langle e_g^* \right\rangle, \left\langle e_r^* \right\rangle$ and $\left\langle e_s^* \right\rangle$. We assume that the data sets represent similar spatial and temporal scales, and their error structure is Gaussian. Note, if the data sets resolve different scales the variance common to the smaller spatial and/or temporal scales are part of the variances of residual errors. These variances, also referred to as the representativeness errors, can be minimized by rescaling all data sets to the scale of the coarsest data set.

3. Results

In this section we present the results of the triple collocation analysis. The data used for this analysis are the daily E-OBS and the monthly GPCC gridded rain gauge data sets, and the 15-minutes weather radar and PP-VNIR precipitation occurrence and intensity data sets. The study is performed for European land for the years 2005, 2006, and 2007. The area restriction is imposed by the criterion of data availability in all data sets. Since the PP-VNIR retrievals are limited to daylight hours (solar zenith angles < 72°), we restricted the study period to the summer months, i.e., May, June, July, and August. During these months the availability of PP-VNIR retrievals over Europe is at a maximum. During winter the PP-VNIR algorithm is less suited for precipitation retrievals over Europe. Beside the very limited number of daylight-only observations with solar zenith angles < 72°, precipitation manifests in more different forms during winter (e.g. convective, stratiform, drizzle, and solid precipitation). During summer the dominant form is convective precipitation. For similar reasons weather radar observations during winter are less reliable than during summer. The weather radar data were used to calculate the ratios between 24-hr and daylight-only precipitation on a pixel-by-pixel basis, which were used to convert the daylight-only PP-VNIR retrievals to 24-hr sums. Wüest et al. (2009) found that diurnal cycles of precipitation, derived from weather radar data that are bias-corrected with daily rain gauge observations, provide accurate diurnal cycles of precipitation occurrence and intensity. Their study confirms that temporal variations in weather radar data may be used to convert the daylight-only values to 24-hr sums.

As stated in Section 3, the main assumptions behind triple collocation are that all datasets are linearly related, and that the errors are Gaussian. These assumptions were tested and shown to hold (results not shown). The three data sets were averaged over sufficiently long periods and re-gridded to sufficiently low resolutions to achieve data sets that are distributed Gaussian. The linearity between the three data sets was verified as well (not shown), and was also shown by Roebeling and Holleman (2009) and Wolters et al. (2011).

Spatial errors in the precipitation data sets

To quantify the spatial errors in the precipitation data sets the triple collocation errors, hereinafter referred to as triple-errors, were calculated for the mean precipitation amounts, expressed in mm day^{-1}, over the summer months of 2005, 2006, and 2007. The weather radar and PP-VNIR data sets were re-sampled to the spatial resolution of the data sets with the coarsest resolution, which is 0.50x0.50° in case the GPCC data set is used and 0.25°x0.25° in case the E-OBS data set is used. As an example Figure 1 presents the spatial distributions of the precipitation amounts over the summer months of 2006, as derived from the E-OBS, PP-VNIR and weather radar data sets. These types of data sets (images) were generated for the summer months of 2005, 2006, and 2007. For each year of summer months a single triple-error can be calculated from three of these data sets, which is representative for the spatial coherence between these data sets for the entire observation domain and period of summer months. The triple-errors and data sets statistics are presented in Table 1 taking E-OBS as a reference, and Table 2 taking GPCC as a reference.

A qualitative analysis of this Figure 1 reveals large differences between the three data sets. Especially the weather radar data deviate much from the other two data sets, and seem to be wetter over major parts of France and drier over major parts of the UK as compared to the other data sets. These differences are in agreement with the results of Lopez (2008) and Kidd et al. (2011), who found that the OPERA precipitation radar composite exhibit systematic and consistent differences with respect to CMORPH, rain gauge, and European Centre for Medium-Range Weather Forecasts (ECMWF) model data sets. They found that the OPERA precipitation radar composite observes more precipitation over France and the North Sea, while a strong deficit is observed over the UK.

Although the spatial patterns of the E-OBS and PP-VNIR data sets are similar, the absolute precipitation amounts of E-OBS are systematically lower than the PP-VNIR amounts. This is confirmed by the statistics presented in Table 1 and Table 2. Compared to E-OBS, the median precipitation amounts of PP-VNIR and weather radar are respectively about 0.75 and 1.25 mm day^{-1} higher, while they are respectively about 0.45 and 1.00 mm day^{-1} higher for GPCC. It is noteworthy that there is a bias of about 0.25 mm day^{-1} between the median precipitation amounts of GPCC (Table 1) and E-OBS (Table 2). This bias may be explained by differences in quality control procedures (van den Besselaar et al., 2011), and by differences in the number of observing stations and in the interpolation method that is used to prepare the data sets (Hofstra et al., 2009). The GPCC data set is likely to be more accurate over Germany and France, where many more observing stations contributed to GPCC than to E-OBS. The correlations, which were calculated relative to the E-OBS or GPCC data sets, show that the PP-VNIR retrievals correlate fairly well with these data sets, better than 0.62 for E-OBS and better than 0.71 for GPCC, whereas the weather radar data correlate very weakly with these data sets. The triple-errors of E-OBS, GPCC, and PP-VNIR, are of the same order of magnitude, and never exceed 1.0 mm day^{-1}. PP-VNIR consistently has smaller errors than the weather radar observations. It also has smaller errors than E-OBS and GPCC for one of the three years.

The high triple-errors in the weather radar data have three reasons. First, the weather radar composite is constructed from observations of a network of 59 weather radars. Making a reliable European composite requires very good harmonization between these radars. This is difficult to achieve because the network comprises different types of radars (see Section 2), operated by 6 different European meteorological services. It implies that there are different detection thresholds, clutter filters, and calibration procedures as well as different operational practices. This may cause differences between radars (and especially countries) in retrieved rainfall. In addition, Lopez (1998) found that part of the observed differences resulted from errors in the post-processing procedures that are used to prepare the data for OPERA. Currently, one of the main focuses of the OPERA program is to improve harmonization and data quality of radars across Europe (see Section 2). Second, the radar signal is a function of distance from the radar and the terrain type, which can cause spatial biases in the observations. Third, the radar observations might be corrupted by clutter. Although sophisticated procedures to remove clutter have been applied by radar operators, a few missed events can still affect the maximum and standard deviation values of the weather radar products. This is confirmed by the high maximum rain amounts from weather radar presented in Table 1 and Table 2.

Temporal errors in the precipitation data sets

To quantify the temporal errors in the precipitation data sets, the triple-errors were calculated per grid box for the decadal (10 days) precipitation amounts during the summer months of 2005, 2006, and 2007. The decadal precipitation amounts from weather radar and PP-VNIR were re-sampled to the spatial resolution of 0.25°×0.25° of the E-OBS data set. Note that the statistics presented in this sub-section (e.g. the correlations in Figure 2 and the triple-errors in Figure 3) were calculated for each re-sampled grid box separately. These statistics represent the temporal relationship between the three data sets at a specific location only, and were calculated from 36 decadal precipitation values of the three data sets for that grid box.

The triple collocation method only provides meaningful error estimates if the considered data sets represent the same physical quantity and are sufficiently correlated. This is verified by evaluating the correlations between the three data sets. Figure 2 presents the spatial distributions of correlations between decadal precipitation amounts from weather radar and E-OBS, from PP-VNIR and E-OBS, and from weather radar and PP-VNIR. This figure shows that the weather radar is highly correlated with the E-OBS data. The 10^{th} and 90^{th} percentiles of the correlations are 0.39 and 0.83. As expected, an offline evaluation of the sampling density of the rain gauges revealed that the areas with the highest correlations correspond to areas with the densest sampling, while the correlations are lower in coarser sampled and mountainous areas. The correlations between PP-VNIR and E-OBS are weaker; the 10^{th} and 90^{th} percentiles of the correlations are 0.34 and 0.69. These values are close to the values found for the spatial error analysis (see Table 1). The PP-VNIR correlates better with the weather radar data, with 10^{th} and 90^{th} percentiles of the correlations of 0.42 and 0.76.

Figure 3 presents the triple-errors of the E-OBS, weather radar, and PP-VNIR data sets. This figure shows that the issues of weather radar observations regarding clutter and harmonization that greatly affect the spatial variations in precipitation amount have much less effect on temporal variations in precipitation amount on a sub-monthly scale. This can be seen from small triple errors in the weather radar and E-OBS data sets, which vary between 0.5 and 1.5 mm day^{-1}. The errors in the PP-VNIR data set are higher, and range between 1.0 and 2.0 mm day^{-1}. These errors are close to the values that we found for the analysis of spatial errors. The strengths and weaknesses of the PP-VNIR algorithm for capturing temporal and spatial variations are similar. Given the fact that this cannot be said for weather radar, the PP-VNIR algorithm is shown to be a valuable new source of precipitation data. This is a major advantage of using a data from a single-platform instrument (i.e. SEVIRI).

Evaluation of the daylight-only diurnal cycle

Information on the daylight-only diurnal cycle of precipitation occurrence and intensity is very important for model evaluations. In this subsection, the diurnal cycles of precipitation occurrence and intensity, as retrieved from weather radar and PP-VNIR observations during daylight hours, are examined in relation to prevailing atmospheric conditions. This examination is done for four subdomains, namely the Atlantic Ocean (ATL), France (FRA), Benelux (BNL), and Germany (GER). These subdomains represent different climate zones i.e., in subdomain FRA a summer convection climate with influence from the Atlantic Ocean; in subdomain BNL a Maritime climate; in the subdomain GER a humid continental climate; and in subdomain ATL an oceanic climate. Figure 4 presents the location of these subdomains. In the previous sub-sections we have shown that the network of weather radars has great difficulty in capturing spatial variations in precipitation amounts, whereas it is well capable of capturing decadal variations in precipitation amounts. Hence, it is more useful to normalize the daylight-only diurnal cycles, and analyze the standardized anomalies rather than the absolute differences. The normalized daylight-only diurnal cycles are calculated with the following equation:

$$NDP_t = \frac{R_t}{\frac{1}{n}\sum_{t^{'}=1}^{n} R_{t^{'}}} - 1 \qquad (8)$$

where NDP is the fractional deviation from the mean (between –1 and n-1), R_t is the precipitation occurrence in % or intensity in mm hr^{-1} at time t, and n is the number of observations during the day.

Figure 5 present the daylight-only diurnal cycles of normalized precipitation occurrence and intensity for the selected subdomains. The rain occurrence daylight-only diurnal cycles from weather radar and PP-VNIR are very similar, as can be seen from the high correlations (> 0.77) and low standard deviation of the relative differences (< 0.06). The daylight-only diurnal cycles of precipitation intensities from weather radar and PP-VNIR have lower correlations (between 0.25 and 0.87) and higher standard deviations of the relative differences (< 0.26) than the precipitation occurrence cycles. It can be seen that the largest differences occur in the early morning and late afternoon. It is suggested that these differences originate from higher sensitivity of the cloud microphysical property retrievals to errors. It has been shown in several studies that cloud physical property retrievals at slant solar and/or satellite zenith angles are very sensitive to retrieval errors (Loeb and Coakley 1998, Varnai and Marshak, 2007; Jonkheid et al., 2011). Especially for clouds with large optical thickness these errors can become very large (> 100%). Remarkably, infrared based retrievals also reveal a time lag in precipitation intensity at the end of the day. However, in the case of infrared based retrievals this time lag is caused by the cirrus clouds connected to convective clouds, which can persist for some hours after a convective cloud has dissipated (Gang et al., 2006).

There are distinct differences between the daylight-only diurnal cycles of precipitation occurrence of the four subdomains. Over ocean (subdomain ATL) a typical stratocumulus related cycle is observed, similar to corresponding cycles over Ocean surfaces found from other data sets (Negri et al., 2002; Nesbitt and Zipser, 2003; and Dai et al., 2008. The highest probability of rain occurs at the end of the night. During the day the stratocumulus clouds start to dissolve, which is revealed by a decreasing probability of rain as the day progresses. Over land the summertime daylight-only diurnal cycles of the precipitation properties are dominated by convective clouds that strongly respond to the daylight-only diurnal cycle of the land surface temperature. During the night, the land surface cools down and convective cloud systems collapse. During the day, the surface heats up and convective processes start to develop. The strongest convection is typically found in the afternoon when surface temperatures are highest. The daylight-only diurnal cycles of precipitation occurrence over the three terrestrial subdomains show remarkably similar patterns, with 20% lower occurrences in the morning and 20% higher occurrences at the end of the day. These variations are in line with the findings of Levizzani et al. (2010), who found from infrared observations that the percentage of cold clouds over Europe land increases by about 50% from 8 – 16-h UTC. The daylight-only diurnal cycles of precipitation intensity over these subdomains exhibit a pronounced peak in intensity in the afternoon. Compared to the morning, the afternoon intensities are about 70% higher over subdomain GER, and about 50% higher over subdomains BNL and FRA, according to the radar data. The sharp increase in precipitation intensity over continental Europe (subdomain GER) suggests that the summertime weather over this subdomain is dominated by convection. The global mean diurnal cycle of precipitation over land from CMORPH data, as presented by Janowiak et al. (2005), shows a similar shape but a smaller increase from 8 - 16 h (~30%), than the daylight-only diurnal cycles presented in Figure 5. The latter is confirmed by Wolters et al. (2011), who compared PP-VNIR and CMORPH daylight-only diurnal cycles of precipitation intensity over West Africa, and found that these cycles had similar shapes, but revealed a larger increase from morning till afternoon for PP-VNIR than for CMORPH, which may be related to the better spatial and temporal resolution of the SEVIRI instrument.

4. Summary and conclusions

In this paper the triple collocation method is applied to estimate spatial and temporal triple-errors in three precipitation data sets, i.e., gridded rain gauge (E-OBS and GPCC), weather radar, and PP-VNIR precipitation data sets. The large number of coinciding observations in these three data sets allows for a statistical assessment of the accuracy and precision of these types of information over Europe. The potential of using the PP-VNIR algorithm for precipitation occurrence and intensity retrievals from SEVIRI is shown. It is discussed that the weather radar composites face a number of shortcomings related to clutter and harmonization of the radar network with respect to obtaining spatially consistent distributions of precipitation amounts, whereas weather radar observations appear very well suited for monitoring temporal variations in precipitation.

The results show that the spatial triple-errors are smaller than 1.0 mm day^{-1} for the gridded rain gauge and PP-VNIR data sets. However, the spatial triple-errors in the European weather radar composite are very large (up to 18 mm day^{-1}) and the correlation to the other data sets is close to zero. It is argued that techniques to composite weather radar observations need major improvements, e.g., by harmonizing algorithms, intercalibrating instruments and improving distance correction procedures, before a spatially consistent European composite of precipitation amount can be generated from weather radar. In contrast, the analysis of temporal triple-errors reveals that weather radars are capable of capturing temporal variations. Apart from the mountainous areas, the temporal triple errors are smaller than 1.0 mm day^{-1}.

It is shown that the daylight-only diurnal cycles of the precipitation occurrence retrievals from weather radar and PP-VNIR agree very well over European climate regions, with correlations between 0.8 and 1.0. Although the correlations of these cycles are lower for precipitation intensity they still range between 0.3 and 0.9, which is reasonable. It is argued that these differences are related to the fact that the SEVIRI retrievals experience saturation for very thick clouds or during the unfavorable viewing conditions that occur during early morning or late afternoon. A disadvantage of the PP-VNIR algorithm is that the retrievals can only be carried out during daylight hours. However, PP-VNIR retrievals can be made from observations of geostationary satellites, such as MSG, at an unprecedented sampling rate of 15 minutes for one fifth of the globe over land and ocean surfaces. This makes these retrievals a valuable source of information for water and energy balance studies.

This paper shows that the triple collocation technique is a promising method to estimate the errors in precipitation data sets. The magnitudes of the spatial and temporal triple-errors are reasonable and can be explained by performance issues of each data set. The observed differences in the spatial triple-errors reveal serious issues related to the aggregation of weather radar observations. This confirms the need for harmonization and quality control and improvement of radar data across Europe, which is currently one of the main focuses of the OPERA program. The observed patterns in the temporal triple-errors reveal larger triple-errors in the under-sampled regions of the E-OBS data sets as well as in mountainous areas. Moreover, these errors show the lower ability of PP-VNIR relative to E-OBS and weather radar to monitor temporal variations in precipitation. Although triple collocation is a powerful method, it should be realized that this approach cannot be applied blindly. Two assumptions are central for the validity of the derived error model. Firstly, the residual errors need to be uncorrelated. Secondly, there need to be linear relations between the data sets. The first assumption is true because the three data sets used in this study are derived with fundamentally different observation techniques and retrieval methods. However, systematic spatial correlations may occur due to different regional uncertainties in the data sets. The second assumption is not necessarily true. Although the three data sets represent the same physical quantity, their measurement methods observe precipitation at different altitudes and sampling resolutions. Due to the latter differences, a more sophisticated calibration approach might be necessary to minimize systematic errors.

In the future, the improvement of precipitation predictions in hydrostatic and non-hydrostatic NWP models would be a very valuable step towards better forecasting of extreme weather events, such as the area, intensity and lifetime of severe rainstorms. Until recently, only weather radars could provide the frequent precipitation observations required to evaluate precipitation predictions. Upcoming radars on the European Space Agency (ESA) Earth Clouds, Aerosols, and Radiation Explorer (EarthCARE), and the three-hourly observations that will be provided by the Global Precipitation Measurement (GPM) era constellation of satellites are important steps towards more frequent availability of accurate precipitation data (Kidd et al., 2010) through an improved understanding of the microphysical properties of the hydrometeors and of the vertical cloud and rain column (e.g., Barker et al., 2011; Iguchi et al., 2010). However, the single-sensor PP-VNIR algorithm is unique because it combines the strong points of different methods that were developed for different satellite instruments (passive microwave and passive imagers), and it provides precipitation retrievals over land and ocean at a 15-minute time resolution without the necessity of using additional information. Because the PP-VNIR retrievals are not corrected with other observations, the original precipitation statistics are conserved. Provided these statistics are realistic they would be of great value for model evaluation studies, while data sets such as CMORPH and GPCP are less suitable for such studies.

5. ACKNOWLEDGEMENT

This work was part of the Water Cycle Multi-mission Observation Strategy (WACMOS) project co-sponsored by ESA and the EUropean Reanalysis and Observations for Monitoring

(EURO4M) project co-sponsored by the European Union. We thank Else van den Besselaar and Wouter Greuell for their comments on earlier version of this manuscript. Further, we want to thank Wouter Dorigo for providing the triple collocation code and Ad Stoffelen for taking the time to explaining the triple collocation technique in more detail. Finally, we acknowledge the OPERA program, and in particular Iwan Holleman, for providing the European weather radar data.

6. REFERENCES

Adler, R. F., and A. J. Negri, 1988: A satellite IR technique to estimate tropical convective and stratiform rainfall. *J. Appl. Meteorol.*, **27**, 30-51.

Adler, R.F., G.J. Huffman, A. Chang, R. Ferraro, P. Xie, J. Janowiak, B. Rudolf, U. Schneider, S. Curtis, D. Bolvin, A. Gruber, J. Susskind, P. Arkin, E. Nelkin 2003: The Version 2 Global Precipitation Climatology Project (GPCP) Monthly Precipitation Analysis (1979-Present). *J. Hydrometeor.*, **4**,1147-1167.

Barker, H. W., M. P. Jerg, T. Wehr, S. Kato, D. P. Donovan, and R. J. Hogan, 2011: A 3D cloud-construction algorithm for the EarthCARE satellite mission. *Quart. J. Roy. Meteor. Soc.*, **137**, 1042-1058.

Battan, L.J., 1973: *Radar Observations of the Atmosphere*. University of Chicago Press, 324 pp.

De Haan, J. F., P. Bosma, and J. W. Hovenier, 1987: The adding method for multiple scattering calculations of polarized light, *Astron. Astrophys.*, **183**, 371-391.

Dai A., X. Lin, and K.-L. Hsu, 2007: The frequency, intensity, and diurnal cycle of precipitation in surface and satellite observations over low- and mid-latitudes, *Clim. Dyn.*, **29**, 727–744, DOI 10.1007/s00382-007-0260-y

Doviak, R.J., and D.S. Zrnic, 1993: *Doppler radar and weather observations*. 2nd edition, Academic press, 562 pp.

Dorigo, W.A., K. Scipal, R.M. Parinussa, Y.Y. Liu, W. Wagner, R.A.M. de Jeu, and V. Naeimi, 2010: Error characterisation of global active and passive microwave soil moisture datasets, Hydrol. Earth Syst. Sci., 14, 2605-2616, doi:10.5194/hess-14-2605-2010.

Hong G., G. Heygster, and C.A.M. Rodriguez, 2006: Effect of cirrus clouds on the diurnal cycle of tropical deep convective clouds, *J. Geophys. Res.*, **111**, D06209, doi:10.1029/2005JD006208, 2006

Grecu, M., and W.S. Olson, 2008: Precipitating snow retrievals from combined airborne cloud radar and millimeter-wave radiometer observations, *J. Appl. Meteorol. Clim.*, **47**, 1634–1650.

Hazenberg, P., H. Leijnse en R. Uijlenhoet, 2011: Radar rainfall estimation of stratiform winter precipitation in the Belgian Ardennes, *Water Resour. Res.*, **47**, 2, W02507, doi:10.1029/2010WR009068.

Haylock, M.R., N. Hofstra, A.M.G. Klein Tank, E.J. Klok, P.D. Jones, and M. New. 2008: A European daily high-resolution gridded dataset of surface temperature and precipitation. *J. Geophys. Res,* **113**, D20119, doi:10.1029/2008JD10201

Hofstra, N, M. New, and C. McSweeney, 2010: The influence of interpolation and station network density on the distributions and trends of climate variables in gridded daily data, *Clim Dyn*, **35**, 841–858, DOI 10.1007/s00382-009-0698-1.

Holleman, I., L. Delobbe, and A. Zgonc, 2008: Update on the European weather radar network (OPERA), *Proceedings of the* 4^{th} *European Conference on Radar in Meteorology and Hydrology*,Helsinki, Finland, June 30-July 4, paper 3.3.

Hsu, K., X. Gao, S. Sorooshian, and H. V. Gupta, 1997: Precipitation Estimation from Remotely Sensed Information Using Artificial Neural Networks. *J. Appl. Meteor.*, **36**, 1176–1190. doi: 10.1175/1520-0450(1997).

Huuskonen, A., 2006: EUMETNET OPERA: operational programme for the exchange of weather radar information. *Proceedings of the* 4^{th} *European Conference on Radar in Meteorology and Hydrology*, Barcelona, September 18-22, p.371-373.

Huuskonen, A., 2010: News on the European weather radar network (OPERA). *Proceedings of the 6th European Conference on Radar in Meteorology and Hydrology*, Sibiu, September 6-10, paper P13.2.

Iguchi, T., S. Seto, R. Meneghini, N. Yoshida, J. Awaka, and T. Kubota, 2010: *GPM/DPR Level-2 Algorithm Theoretical Basis Document*. NASA-GSFC, 72 pp.

Janowiak, J. E., V. E. Kousky, and R. J. Joyce, 2005: Diurnal cycle of precipitation determined from the CMORPH high spatial and temporal resolution global precipitation analyses, *J. Geophys. Res.*, **110**, D23105, doi:10.1029/2005JD006156.

Janssen, P. A. E. M., S. Abdalla, H. Hersbach, and J.R. Bidlot, 2007: Error Estimation of Buoy, Satellite, and Model Wave Height Data. *J. Atmos. Ocean. Technol.*, **24**, 1665–1677.

Jonkheid, B.D., R.A. Roebeling, and E. van Meijgaard, Quantifying uncertainties of cloud physical properties derived from simulated SEVIRI observations, *Atm. Chem. Phys.* (submitted).

Joyce, Robert J., John E. Janowiak, Phillip A. Arkin, and Pingping Xie, 2004: CMORPH: A Method that Produces Global Precipitation Estimates from Passive Microwave and Infrared Data at High Spatial and Temporal Resolution. *J. Hydrometeorol.*, **5**, 487–503.

Kidd, C., R. Ferraro, and V. Levizzani, 2010: The Fourth International Precipitation Working Group Workshop, *B. Amer. Meteor. Soc.*, **91**(8), 1095–1099, doi:10.1175/2009BAMS2871.1

Kidd, C., and V. Levizzani, 2011: Status of satellite precipitation retrievals. *Hydrol. Earth Syst. Sci.*, 15, 1109-1116.

Kidd, C., P. Bauer, J. Turk, G.J. Huffman, R. Joyce, K-L Hsu, and D. Braithwaite, 2011: Inter-comparison of high-resolution precipitation products over northwest Europe, *J. Hydrometeor.*, doi: http://dx.doi.org/10.1175/JHM-D-11-042.1.

Krajewski, W.F., G. Villarini, and J.A. Smith, 2010: Radar-rainfall uncertainties: where are we after thirty years of effort?, *Bull. Am. Met. Soc.*, **91**(1), 87-94.

Lensky, I. M., and D. Rosenfeld, 2006: The time-space exchangeability of satellite retrieved relations between cloud top temperature and particle effective radius, *Atmos. Chem. Phys.*, **6**, 2887– 2894.

Levizzani, V., F. Pinelli, M. Pasqui, S. Melani, A.G. Laing, and R.E. Carbone, 2010: A 10-year climatology of warm-season cloud patterns over Europe and the Mediterranean from meteosat IR observations. *Atmos. Res.*, **97**, 555-576, 10.1016/j.atmosres.2010.05.014.

Levizzani, V., S. Laviola, and E. Cattani, 2011: Detection and measurement of snowfall from space. *Remote Sensing*, 3, 145-166.

Loeb, N. G., and J. A. Coakley Jr., 1998: Inference of marine stratus cloud optical depth from satellite measurements: Does 1D theory apply?, *J. Climate*, **11**, 215–233.

Lopez, P., 2008: Comparison of OPERA precipitation radar composites to CMORPH, SYNOP and ECMWF model data. Tech. Rep., ECMWF Tech. Memo. 569, 22 pp.

Marshall, J. S., W. Hitschfeld, and K. L. S. Gunn, 1955: Advances in radar weather. Advances in Geophysics, Vol. 2, Academic Press, 1–56.

Nauss T., and A.A. Kokhanovsky, 2006: Discriminating raining from non-raining clouds at mid-latitudes using multispectral satellite data. *Atmos. Chem. Phys.* **6**, 5031–5036.

Negri A., J., T. L. Bell, and L. Xu, 2002: Sampling of the Diurnal Cycle of Precipitation Using TRMM. *J. Atmos. Oceanic Technol.*, **19**, 1333–1344. doi: http://dx.doi.org/10.1175/1520-0426(2002)019<1333:SOTDCO>2.0.CO;2

Nesbitt S.W., and E.J. Zipser, 2003: The Diurnal Cycle of Rainfall and Convective Intensity according to Three Years of TRMM Measurements. *J. Climate*, **16**, 1456–1475.

Overeem, A., I. Holleman, and A. Buishand, 2009: Derivation of a 10-year radar-based climatology of rainfall, *J. Appl. Meteorol. Clim.*, **48(7)**, 1448– 1463, doi:10.1175/2009JAMC1954.1.

Roebeling, R.A., A.J. Feijt, and P. Stammes, 2006: Cloud property retrievals for climate monitoring: implications of differences between SEVIRI on METEOSAT-8 and AVHRR on NOAA-17, *J. Geophys. Res.*, **111**, 20210, doi:10.1029/2005JD006990.

Roebeling R. A., H.M. Deneke, and A.J. Feijt, 2008: Validation of cloud liquid water path retrievals from SEVIRI using one year of CloudNET observations , *J. Appl. Meteorol. Clim.*, **47**, 206-222

Roebeling R.A. and I. Holleman, 2009: SEVIRI rainfall retrieval and validation using weather radar observations, *J. Geophys. Res.* , **114**, D21202, doi:10.1029/2009JD012102.

Rosenfeld, D., and G. Gutman, 1994: Retrieving microphysical properties near the tops of potential rain clouds by multispectral analysis of AVHRR data, *Atmos. Res.*, **34**, 259–283, doi:10.1016/0169-8095(94)90096-5.

Rudolf B., A. Becker, U. Schneider, A. Meyer-Christoffer, and M. Ziese, 2011: New GPCC Full Data Reanalysis Version 5, GEWEX Newletter, Vol 21, No 2, May 2011.

Scipal, K., T. Holmes, R. de Jeu, V. Naeimi, and W. Wagner, 2008: A possible solution for the problem of estimating the error structure of global soil moisture data sets, *Geophys. Res. Lett.*, **35**, L24403, doi:10.1029/2008GL035599.

Stammes, P., 2001: Spectral radiance modeling in the UV-Visible range. IRS 2000: Current problems in Atmospheric Radiation, edited by W.L. Smith and Y.M. Timofeyev, pp 385-388, A. Deepak Publ., Hampton, VA.

Stoffelen, A., 1998: Towards the True Near-Surface Wind Speed: Error Modelling and calibration Using Triple Collocation, *J. Geophys. Res.*, **103**, 7755-7766.

Thies B., T. Nauss, and J. Bendix, 2008: Discriminating raining from non-raining clouds at mid-latitudes using meteosat second generation daytime data, *Atmos. Chem. Phys*., **8**, 2341–2349.

Todd, M. C., E. C. Barrett, M. J. Beaumont, and J. L. Green, 1995: Satellite identification of rain days over the upper Nile river basin using an optimum infrared rain/no-rain threshold temperature model, *J. Appl. Meteorol.*, **34**, 2600 – 2611.

van den Besselaar E. J. M., A.M.G. Klein Tank, G. van der Schrier, and P.D. Jones, 2011: Synoptic messages to extend climate data records, *J. Geophys. Res.*, (submitted)

Varnai, T., and A. Marshak, 2007: View angle dependence of cloud optical thickness retrieved by MODIS, *J. Geophys. Res.*, **112**, D06203, doi:10.1029/2005JD006912.

Vicente, G. A., R. A. Scofield, and W. P. Menzel, 1998: The operational GOES infrared rainfall estimation technique. Bull. Amer. Meteor. Soc., 79, 1883-1898.

Wentz, F. J., and R. W. Spencer, 1998: SSM/I Rain retrievals within a unified all-weather ocean algorithm, *J. Atmos. Sci.*, **55**, 1613 – 1627.

Willmott, C.J., C.M. Rowe and W.D. Philpot, 1985: Small-scale climate maps: A sensitivity analysis of some common assumptions associated with grid-point interpolation and contouring. *Am. Cartographer* **12**(1), 5-16.

Wilson, J.W. and E.A. Brandes, 1979: Radar measurement of rainfall – a summary, *Bull. Am. Met. Soc.*, **60**(9), 1048-1058.

Wolters, E. L. A. Roebeling, R. A., and Feijt, A.J., 2008: Evaluation of cloud phase retrieval methods for SEVIRI on Meteosat-8 using ground-based lidar and cloud radar data, *J. Appl. Meteorol. Clim.*, **47**, 1723-1738, doi:10.1175/2007JAMC1591.1.

Wolters, E.L.A., B.J.J.M. van den Hurk, and R.A. Roebeling, 2011: Evaluation of rainfall retrievals from SEVIRI reflectances over West Africa using TRMM-PR and CMORPH, *Hydrol. Earth Syst. Sci.*, **15**, 437-451, doi:10.5194/hess-15-437-2011.

Wüest M., C. Frei, A. Altenhoff, M. Hagen, M. Litschi, and C. Schär, 2009: A gridded hourly precipitation dataset for Switzerland using rain-gauge analysis and radar-based disaggregation. *Int. J. Climatol.* , DOI: 10.1002/joc.2025.

LIST OF TABLE CAPTIONS

TABLE 1. Statistics and triple-errors for spatial variations in precipitation amounts during summer months (May – August) of 2005, 2006 and 2007 for E-OBS, Weather radar and PP-VNIR.

TABLE 2. Similar to Table 1 but then for GPCC, Weather radar and PP-VNIR

TABLES

TABLE 1. Statistics and triple-errors for spatial variations in precipitation amounts during summer months (May – August) of 2005, 2006 and 2007 for E-OBS, Weather radar and PP-VNIR. Note that the correlations (*Corr.*) are calculated against E-OBS.

Data set	*Median* [mm day^{-1}]	*95th %* [mm day^{-1}]	*Std* [mm day^{-1}]	*Err.* [mm day^{-1}]	*Corr.* [-]
2005					
E-OBS	1.76	2.82	0.85	0.53	1.00
Weather radar	3.01	4.98	1.56	19.69	0.04
PP-VNIR	2.84	4.15	1.04	0.75	0.68
2006					
E-OBS	2.03	3.11	0.82	0.63	1.00
Weather radar	3.30	6.09	1.81	2.16	0.34
PP-VNIR	2.77	4.22	0.96	0.82	0.62
2007					
E-OBS	3.06	3.87	0.85	0.91	1.00
Weather radar	4.45	6.99	2.07	6.38	0.13
PP-VNIR	2.85	4.24	1.06	0.12	0.68

TABLE 2. Similar to Table 1 but for GPCC, Weather radar and PP-VNIR

Data set	*Median* [mm day^{-1}]	*95th %* [mm day^{-1}]	*Std* [mm day^{-1}]	*Err.* [mm day^{-1}]	*Corr.* [-]
2005					
GPCC	2.08	3.11	0.87	0.59	1.00
Weather radar	3.05	4.93	1.50	11.54	0.08
PP-VNIR	2.86	3.98	0.97	0.85	0.82
2006					
GPCC	2.34	3.33	0.85	0.62	1.00
Weather radar	3.33	6.18	1.73	2.18	0.35
PP-VNIR	2.77	4.07	0.89	0.57	0.71
2007					
GPCC	3.31	4.34	0.90	0.51	1.00
Weather radar	4.46	6.87	1.95	4.02	0.22
PP-VNIR	2.82	4.13	1.01	0.63	0.74

LIST OF FIGURE CAPTIONS

FIGURES

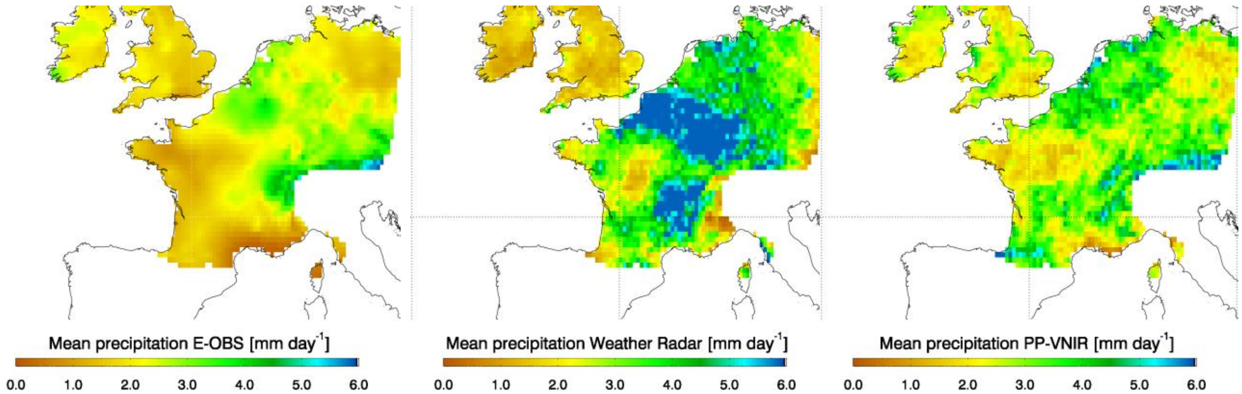

FIG. 1. Example of the mean daily precipitation amounts from E-OBS (left panel), Weather radar (middle panel), and PP-VNIR (right panel) in mm day^{-1} over the period May-August 2006. All data sets are presented at the E-OBS equal latitudinal grid of 0.25°x0.25°. Over the entire domain the mean daily precipitation amounts are 2.12 mm day^{-1} for E-OBS, 3.51 mm day^{-1} for weather radar, and 2.91 mm day^{-1} for PP-VNIR.

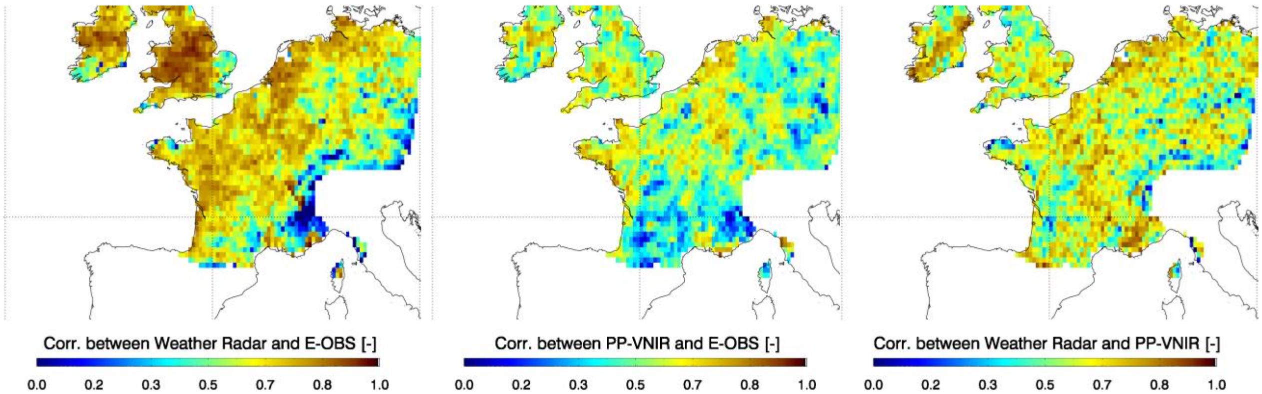

FIG. 2. Correlations between decadal precipitation amounts from Weather radar and E-OBS (left panel), PP-VNIR and E-OBS (middle panel), and Weather radar and PP-VNIR for the summer months (May-August) of the years 2005, 2006, and 2007. All data sets are presented at the E-OBS equal latitudinal grid of 0.25°x0.25°.

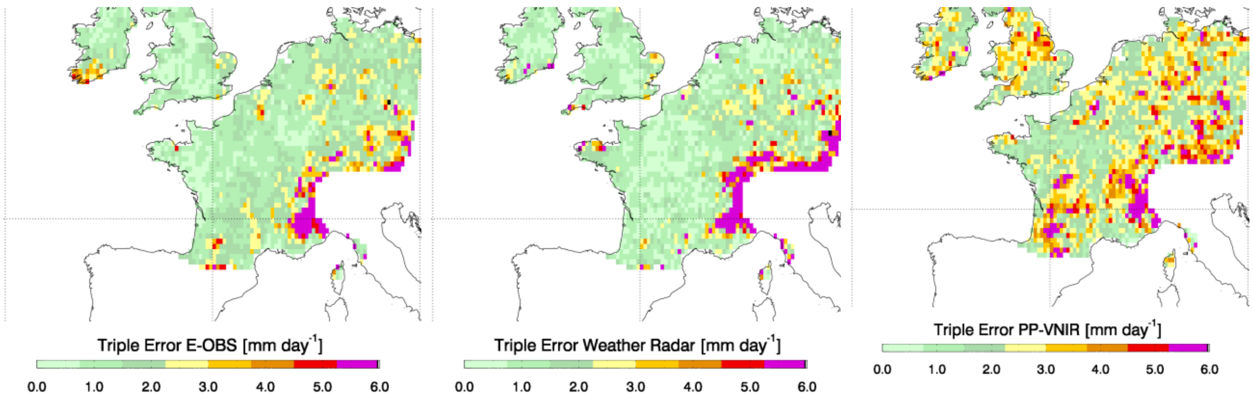

FIG. 3. Triple-errors for temporal variations in decadal precipitation amounts in mm day^{-1} during the summer months (May-August) of 2005, 2006, and 2007 for E-OBS (left panel), Weather radar (middle panel), and PP-VNIR (right panel). All data sets are presented at the E-OBS equal latitudinal grid of 0.25°x0.25°.

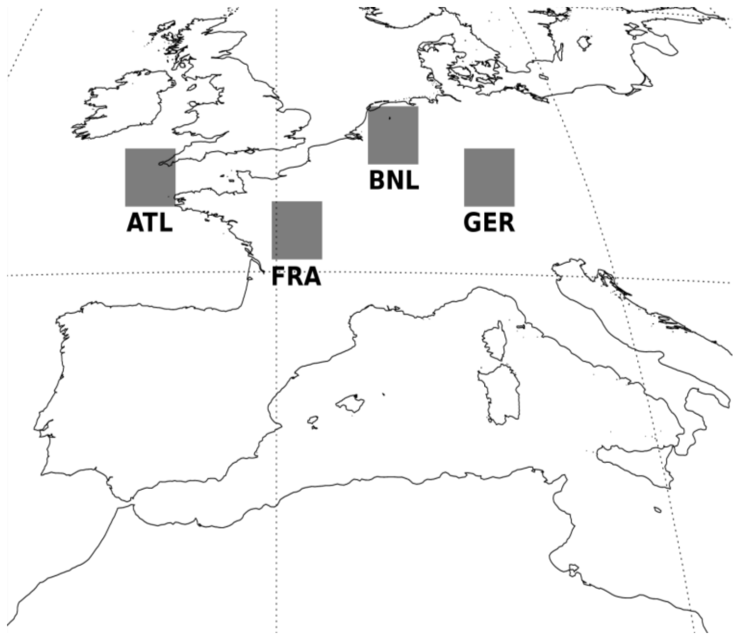

FIG. 4. Location of the subdomains, from left to right Atlantic Ocean (ATL), France (FRA), Benelux (BNL), and Germany (GER)

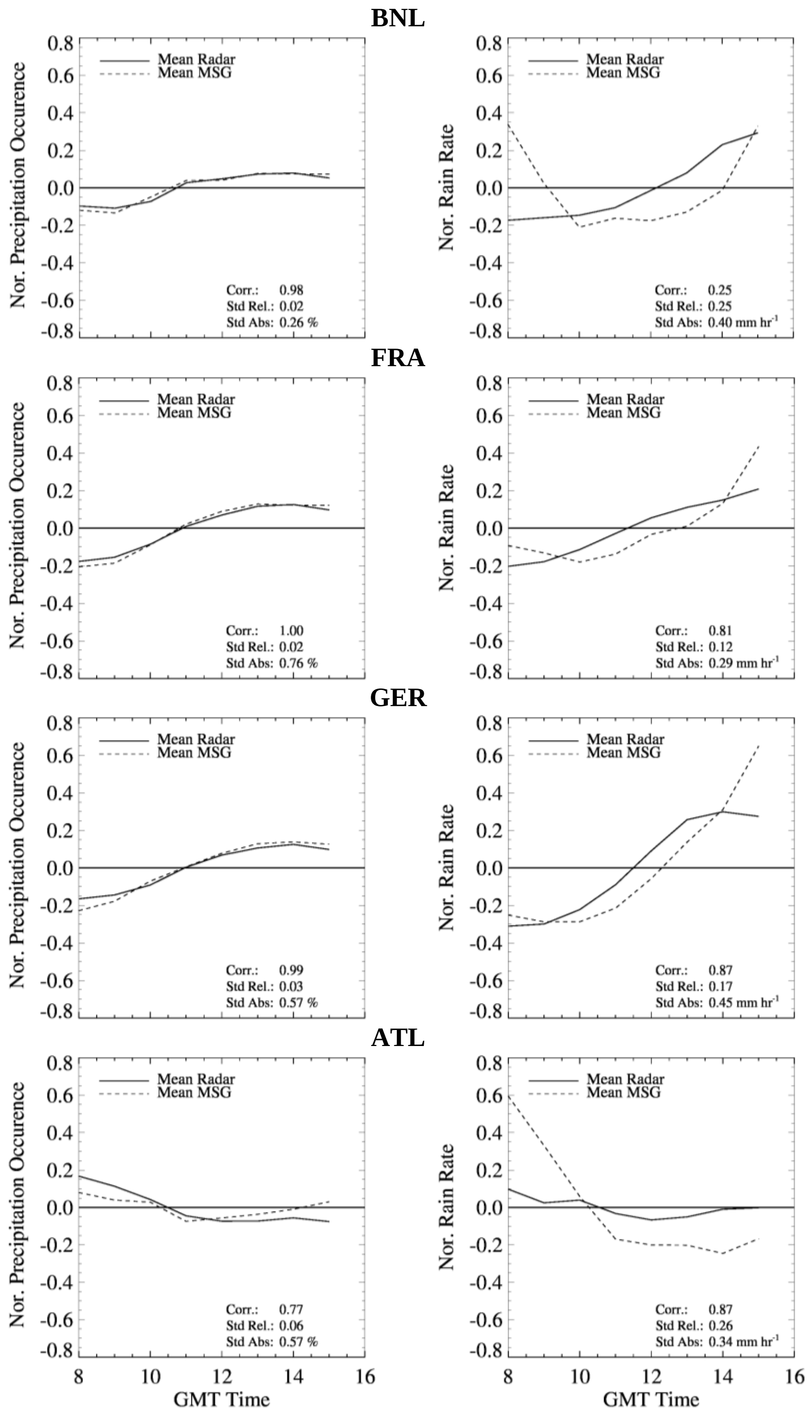

FIG. 5. Normalized daylight-only diurnal cycles of precipitation occurrence (left panel) and intensity (right panel) for the Benelux (BNL), France (FRA), Germany (GER), and Atlantic Ocean (ATL) subdomains, calculated over the period May-August 2005, 2006, and 2007.